Detecting Stellar Radial Velocity through Near-Infrared Spectroscopic Data

Timothy Morrell

A senior thesis submitted to the faculty of
Brigham Young University
in partial fulfillment of the requirements for the degree of

Bachelor of Science

Eric Hintz, Advisor

Department of Physics and Astronomy

Brigham Young University

ABSTRACT

Detecting Stellar Radial Velocity through Near-Infrared Spectroscopic Data

Timothy Morrell
Department of Physics and Astronomy, BYU
Bachelor of Science

Spectroscopic data of the δ scuti star V2455 Cyg collected by the 3.5 meter telescope at Apache Point Observatory (APO) can be used to detect the radial velocities of its pulsation. The *Spextools* software reduces the near-infrared data which can then be analyzed by the FXCOR package located in IRAF where it performs a Fourier cross-correlation. In order to make this data compatible with IRAF, a significant change in the file formatting is required. This paper models different wavelength ranges of the collected spectra to determine which part creates the most accurate radial velocity curves using the known Paschen and Brackett lines. It also compares our derived velocity curves to related data detected in the visible part of the spectrum. As this is the first time that this type of research has been attempted at BYU, there is a discussion of what can be improved on moving forward and how this will open up future, related projects. The results indicate that we are accurately detecting the changing radial velocities from V2455 Cyg's changing spectral absorption lines, but there is a signficant need to improve the error bars moving forward.

Keywords: radial velocity, δ scuti, Fourier cross-correlation, near-infrared spectroscopy, triplespec data reduction, V2455 Cygni

ACKNOWLEDGMENTS

I would like to thank the generous donors of the Physics and Astronomy Department that provide funding for mentored undergraduate research. I also would like to acknowledge the guidance that my advisor, Dr. Eric Hintz, provided throughout the research process and how he has opened my eyes to near-infrared astronomy. Similarly, I am immensely grateful for Scott Call who taught me how to correctly perform research and provided the clear advice of a supportive mentor. Finally, I recognize the enduring support of my wife and family who have shaped me into the person that I am today.

Contents

List of Figures

Chapter 1

Introduction

Astronomers gain a better understanding of stellar atmospheres and interiors by studying pulsating variable stars. These stars transition from the main sequence to become supergiants because they are running out of hydrogen to fuse in their core which creates widespread instability, and the lack of a stable fuel source creates pulsations in the star that are determined by its mass and age. This wide range of variation allows for many different pulsation periods lasting anywhere from a few hours to several months at a time.

The δ scuti star provides considerable information for this research since it can complete an entire pulsation cycle in less than six hours (Handler 2009). Since the star is pulsating so rapidly, it allows astronomers to observe an entire period in the space of a single night. This eliminates needing to piece together the times when a star will be at different parts of its pulsation period over the space of several nights. Since the period is so quick, a δ scuti star will not experience extreme changes in temperature or magnitude.

Other variable stars with longer pulsation cycles include RR lyraes and cepheids. The RR lyraes are the bridge between δ scutis and longer pulsators since their period lasts for the space of a few hours to roughly a day (Lafler & Kinman 1965). Classical cepheid stars can have a period that lasts from a range of roughly one day up to a bit longer than two months. These stars have been focused

on by astronomers over the years since they were studied to determine the Hubble Constant and have been used as standard candles in the distance ladder (Hubble 1988). Stars are studied either with a photometric telescope that uses a high definition camera to count detected photons or with a spectroscopic telescope which is explained in the following section.

1.1 Near-Infrared Spectroscopy

A leading technique in stellar observation is attaching a spectroscopic camera to a telescope that allows for astronomers to directly see a star's blackbody curve. Spectroscopic research allows for a perspective that can't be achieved with photometric techniques since it is possible to directly see spectral absorption and emission features. Spectral features are lines that form in the spectra which are not part of the blackbody curve or caused from noise in the atmosphere. Each of these spectral features are formed from the individual elements that exist within a star, and a star's blackbody curve is as unique as a fingerprint since it is determined by the metallicity, age, mass, and temperature of that specific star. Similarly, spectroscopy can be observed in more than just the visible light spectrum which allows for astronomers to observe different segments of the blackbody curve depending on wavelength.

Over the past few years, astronomy has made a shift towards observing in the near-infrared region of the electro-magnetic spectrum as it has allowed for observation of colder objects and objects with larger redshifts. The TripleSpec instrument (Wilson et al. 2004) used by this research team specifically detects the J, H, and K bands, and it allows for direct observation of both Paschen and Brackett absorption lines. These spectral lines are formed when photons leaving the star collide with a hydrogen atom which then pushes an electron out into a higher energy level. This action absorbs the photons at specific wavelengths creating spectral lines in the blackbody curve which correspond to a known element and energy level. Over the pulsation of a variable star, these lines

are directly impacted as the star changes in size and temperature, and the study of these changing absorption lines allows scientists to peer into the interior structures of stars.

1.2 Research Summary

The goal of this research is to detect the changing radial velocity of a variable star over its pulsation period by observing the changes in spectral lines. This was accomplished by collecting data on a bright δ scuti star known as V2455 Cygni (V2455 Cyg) where nearly two complete pulsation cycles were collected in the space of just under four hours using the 3.5 meter telescope located at Apache Point Observatory. The article, New CCD photometric investigation of high amplitude δ Scuti star V2455 Cyg, (Ostadnezhad et al. 2020) published a known ephemeris for V2455 Cyg which calculates the times when it will be at its peak brightness. The radial velocity values were directly pulled from our collected data using a process known as Fourier cross-correlation derived by (Tonry & Davis 1979) within the FXCOR package of the Image Reduction and Analysis Facility software (IRAF) (Tody 1986). As our team is able to accurately detect the changes in radial velocity this can branch out to support many future projects. The detected radial velocity values will provide deeper understanding of how a variable star evolves than simply observing the photometric changes in brightness of the star.

In the Methods Section of this paper we will explain the observation and reduction processes that allow for clean spectroscopic data even with the challenges of atmospheric interference. The *Spextools* software used in this process was created by (Cushing et al. 2004) and (Vacca et al. 2003). We will then continue to explain how this processed data can be formatted to be compatible with the IRAF software which is able to detect the radial velocity curves using FXCOR. Then in the Results section we will show the radial velocities that were calculated from V2455 Cyg and plot our data with related radial velocity curves. In the Discussion section we will compare these values

to similar data and discuss the potential future projects that can stem off of accurately detecting stellar radial velocities.

Chapter 2

Methods

Our research group collects data using the 3.5 Meter telescope located at Apache Point Observatory (APO) which is part of the Astrophysical Research Consortium. This telescope is equipped with the TripleSpec instrument which is a near-infrared spectrograph that can detect wavelengths in a range of 0.95-2.46 μm. Observations were completed remotely using the Telescope User Interface software (TUI) to directly access the telescope's controls. Figure 2.1 is an image of the 3.5 meter telescope used by this research group at APO, and the instruments used with the telescope can be seen located in the far side of the observing deck.

We observed the known δ scuti star V2455 Cyg on July 3, 2022 for an entire half night which lasted just under four hours. The collected data covered nearly two complete periods of V2455 Cyg which means we detected the star at two separate points of maximum brightness and the one point of minimum between them. In order to confirm that the collected data was accurate, the A0 type star, HD 199217, was also observed throughout the night to be used as a standard star in the data reduction process. HD 199217 was selected since it has a very similar airmass to V2455 Cyg, and since it is defined as an A0 spectral type which means it has very few spectral features and closely resembles a blackbody curve.

Figure 2.1 3.5 meter telescope located at Apache Point Observatory. The observing mirror collects the light and focuses it onto the secondary mirror centered in front of the mirror. The large metal structure directly in front of the observing mirror are the lamp lattices used to take calibration images.

2.1 Reduction Process

Spectroscopic data reduction involves using a program titled *Spextools*, and the recent senior thesis written by Conner Scoresby explains the complete process of learning how to use this data reduction software in minute detail (Scoresby et al. 2023). The focus of this paper is to explain the data reduction process in a broad, general sense, but it will mainly focus on some of the finer details that have been improved on recently which results in overall cleaner spectral curves instead of functioning as a user manual.

2.1.1 Creating Calibration Frames

Earth's atmosphere creates considerable noise that impacts the quality of near-infrared data. The data reduction process attempts to clean and preserve as much noisy data that has been directly

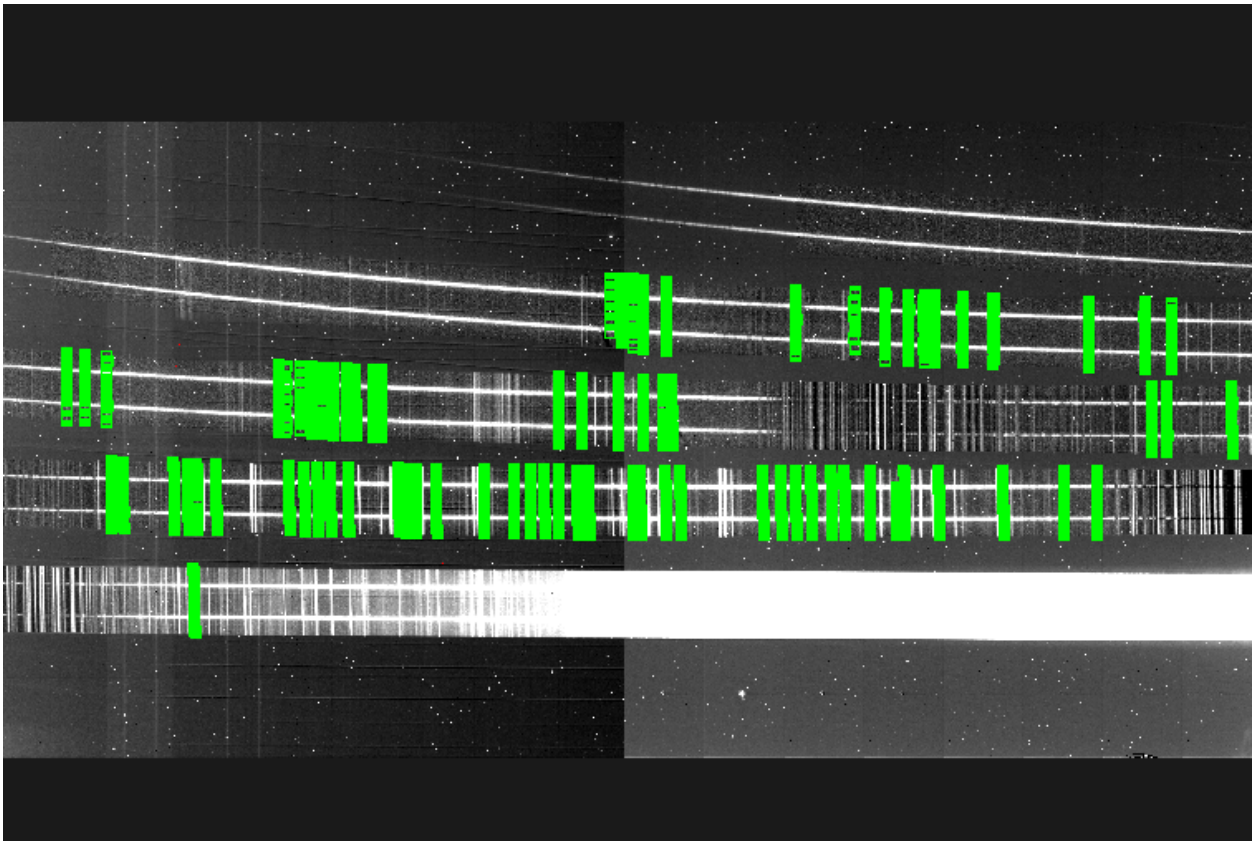

Figure 2.2 Wavelength calibration window which depicts atmospheric lines that have been detected by the bright green vertical lines. The wavecal file will then use these detected atmosphere lines to subtract them from the raw images in the data reduction process

influenced by the atmosphere. The main goal in this process is to limit the atmosphere's impact in our data and to reduce the raw image files into reliable and clean spectra. Our research group has found that using a good wave calibration file can extract information from otherwise unusable data.

We use the wave calibration file known as a wavecal to detect common atmospheric lines that consistently appear and to subtract them from the data since we only want the light of our observed star. Earlier work performed by (Scoresby et al. 2023) has referenced the ability to detect a maximum of 125 atmospheric lines in their data while our group found objects with closer to 145 lines. Figure 2.2 demonstrates the atmospheric lines that are being removed by the wavecal file. By way of experimentation, we have been able to conclude that a wavecal is most likely to be

successful when it is created using data with longer exposure times. Selecting exposure times of roughly 100 to 120 seconds has consistently created the best wavecal files since any longer time will result in the conditions of the sky changing between the start and the end of the photo being taken.

When an effective wavecal file has been found, it can be used for more than a single night of reductions. Our group has determined that since the wavecal is subtracting the influence of the night sky from the images, it does not change dramatically over extended periods of time. With this conclusion we have been able to use the same wavecal file for up to six months with no impact of the quality of the data being reduced.

The second type of calibration frame that is used to help process the data are the flat images which are compiled to form a single master flat file. The purpose of using flats in the data reduction process is that it helps to eliminate any vignetting or dust on the telescope that might interfere with the actual data. Flat images are calibrated by using bright quartz lamps that are attached to the trusses of the telescope, and they are generally taken either at dusk or dawn when it is too bright to be observing.

2.1.2 Data Extraction

Once both a master flat and wavecal file have been created, *Spextools* extracts data through a process of subtracting one image from another to remove the light of the sky that exists in the raw image files. Light is detected by the telescope since it works specifically in the near-infrared where the heat of the sky produces light that is detected, but we only want the light of the observed star. The observation process resolves this issue by alternating between two different points on the telescope slit when collecting data of a single target, and this allows for the reduction process to make a subtraction between two images without losing data. Figure 2.3 demonstrates how the subtraction process creates a positive and negative flux of the two different images and effectively removes any light from the sky in the background.

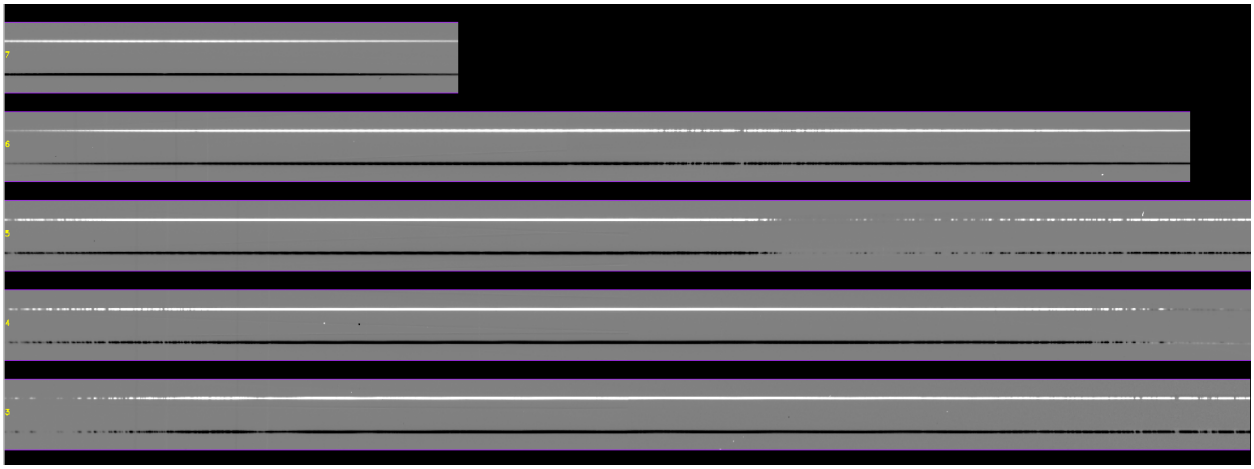

Figure 2.3 Subtraction between two raw images where the background is removed from the images and there exists a positive and negative flux for each star.

This subtraction process is used for every image taken in the night, and the next step is to combine the extracted spectra into a single combined spectra. The benefit of combining multiple spectra is that it is possible to average out the differences between each one to create a single file with the lowest signal-to-noise ratio as possible. We have found that the minimum number of images you can use with a satisfactory signal-to-noise ratio is four. The Figure 2.4 demonstrates how the *Spextools* software can blend all of the different spectroscopic data together without removing actual features from the observed target. The combining process also removes the risk of having a cloud or other issue ruin the data since it is creating a single spectra over a longer period of observation time. With this step completed it is now possible to move into the most time intensive step, which is performing a telluric correction of the data.

2.1.3 Removing atmospheric lines

A key principle of the observation process is that every star that is observed throughout the night should have a corresponding standard star which will be used in the telluric correction process. The standard star is a star that has an airmass as close as possible to the first star and has an A0 spectral

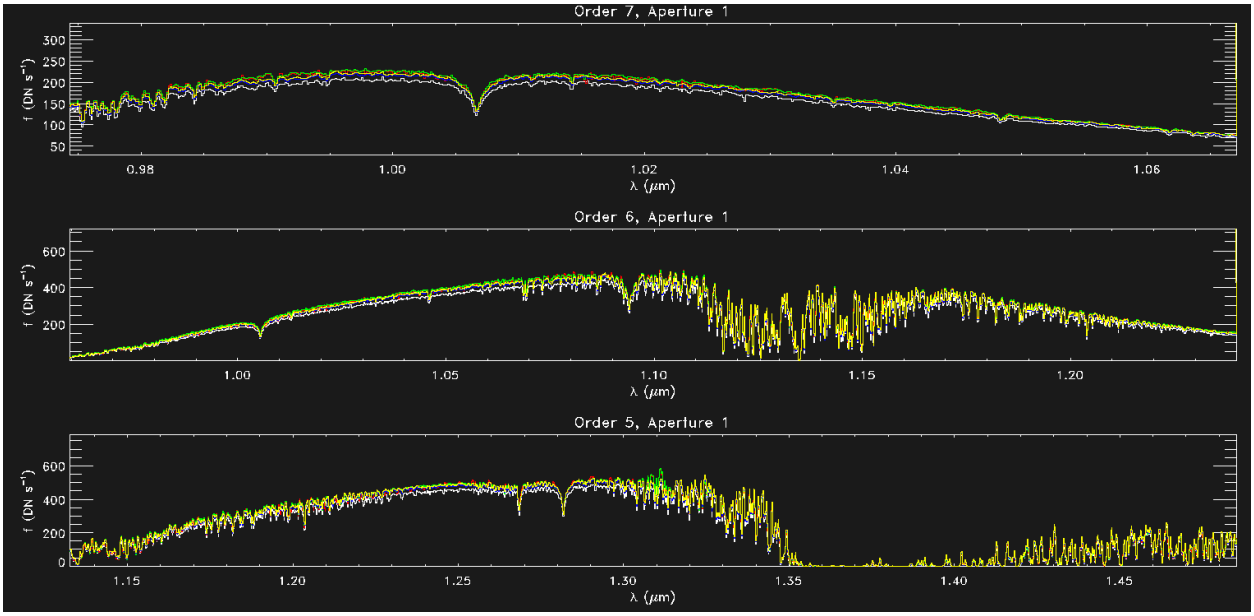

Figure 2.4 Combination of several separate spectroscopic data files in order to create a single spectra that limits the signal to noise in the data.

type. The two stars having the same airmass helps to make sure that they will be comparing the same part of the sky, and the A0 star is extremely valuable since it provides an extremely clean spectra with only a few hydrogen absorption lines. With combined spectras of both an object and a standard star, it is now possible to use the data together to eliminate the atmospheric influence in the data.

The telluric correction occurs by creating a model built from the curve of the standard star and then stretching out the object star to fit the standard star's model. This helps to clean the data since it better aligns spectral features at the right wavelength, can pinpoint known places where the atmosphere makes the data noisy, and try to cut out the influence of the star. The most useful tool in this process is the find shifts window located in *Spextools*, and it can be seen in Figure 2.5. Find shifts performs a pixel shift which is able to directly cut out significant amounts of noise. It is valuable to use find shifts in nearly every instance since it creates such clean data, but when reducing data to detect radial velocities the pixel shift will mask the changes in spectral lines which

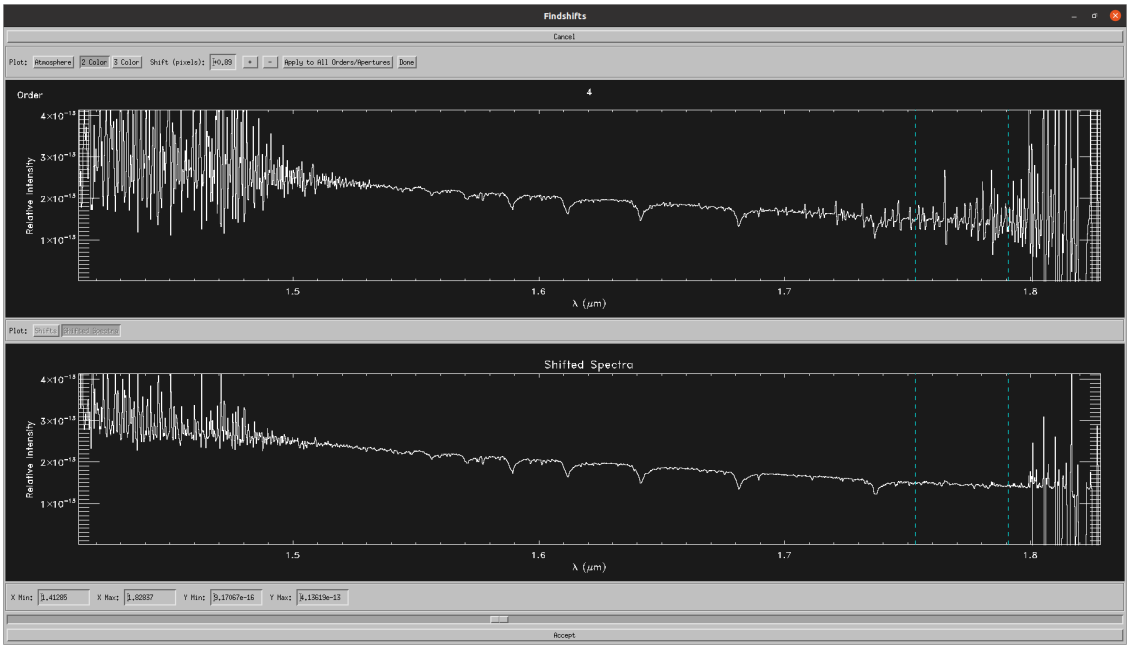

Figure 2.5 Find shift process that performs a pixel shift of the data in order to eliminate known noise from the data. The top graph depicts the data that has not been shifted, and the bottom graph shows the change that takes place in that exact same data once find shifts has been used.

would be used to calculate accurate radial velocity values. It is easier to detect radial velocities with data that contains noise instead of one where the spectral lines have been shifted.

2.1.4 Creating merged data

The final step in the data reduction process is to create a merged file of the spectra that can be used for future analysis and is effectively the end goal of the reduction process. At this step, there are still some parts of the data that are so saturated by the atmosphere's influence that the only possible solution is to cut them out because they provide no value to research. Figure 2.6 shows the spectroscopic data with the white line, and the places where the atmosphere is directly impacting the data demonstrated with the yellow line. By cutting out the noisy data, this will naturally create three large gaps in the data that separate the J, H, and K bands.

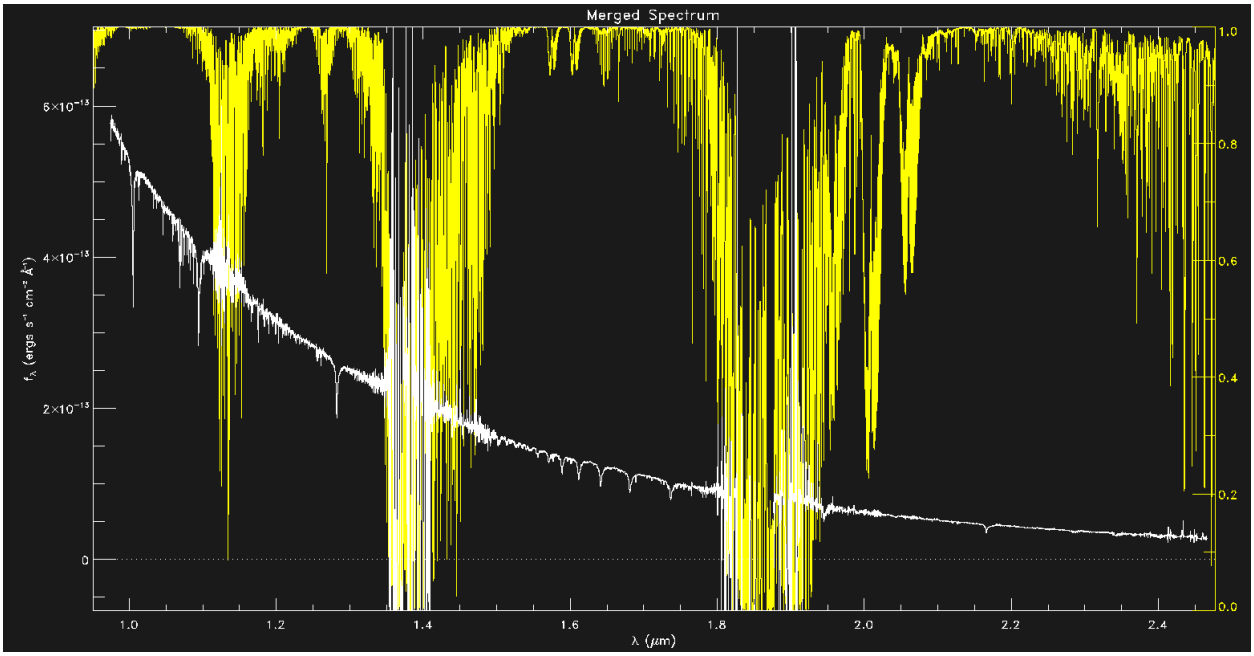

Figure 2.6 Merge orders window where sections of data that are saturated with atmospheric noise are cut from the spectra.

One final comment in the data reduction process is that it is possible to directly convert merged .fits files directly into .text files using the spex2text command in the idl environment located in the terminal window. By converting to a .text file you gain direct access to the data which is much more difficult in a .fits file. Unfortunately, data produced in *Spextools* is not directly compatible with IRAF and the following section explains the process of altering the formatting to be used in both softwares. In order to analyze the data, it is crucial to go through the complete conversion process.

2.2 Determining Radial Velocities from Spectra

In order to analyze the radial velocities from the spectra, the most significant challenge is altering the data to be compatible with the IRAF software. No published information exists of this process, so the following method was conceived by the author and assuredly there is a more effective approach using a code to automate the process.

Both *Spextools* and IRAF use the same file type which is a .fits file, but that does not allow for files to be immediately compatible with both software since a .fits file can have different dimensions depending on the number of data columns contained within the file. Through trial and error, the easiest technique is to start by opening an IRAF window that is located in the file with the data, and then use the SCOPY command which is located in the ONEDSPEC package shown in Figure 2.7. The parameters for SCOPY must be changed beforehand for it to work though, and it is important to change the format of the spectra to be onedspec instead of multispec. This step is taking the .fits file and separating each column of data into four separate files which allows us to access the data that we need. The different files produced in order are the wavelengths, detected flux, sound-to-noise ratio, and finally a list of zeros. IRAF can read the file only if it contains the first two files which are the wavelengths and flux.

In order to recombine the two data files into a format usable with IRAF, there is another step which is converting them into .text files that allows us to directly access the data located in the files. Luckily, IRAF provides another command in the ONEDSPEC package which is called WSPECTEXT which directly makes this conversion. In order to complete this next step, I uploaded the two .text files we just made with WSPECTEXT into an Excel sheet that allowed me to directly move the data in a much easier fashion. Once the data is located in Excel, the first step is to erase the headers created by *Spextools* since it is one of the key problems that makes it incompatible with IRAF. Next, the wavelengths need to be converted into angstroms since *Spextools* produces them in microns, and this can be done by multiplying the entire wavelength column by a value of 10,000. Finally, this process is complete when there are only two columns in the Excel file with the left one being the wavelength in angstroms and the right column being the flux of the spectra.

The final step of converting the data back into a .fits file is relatively straightforward since it is completed by saving this Excel document back into a .text file. Then IRAF can make the conversion using the RSPECTEXT command which will now make it compatible with all packages on IRAF.

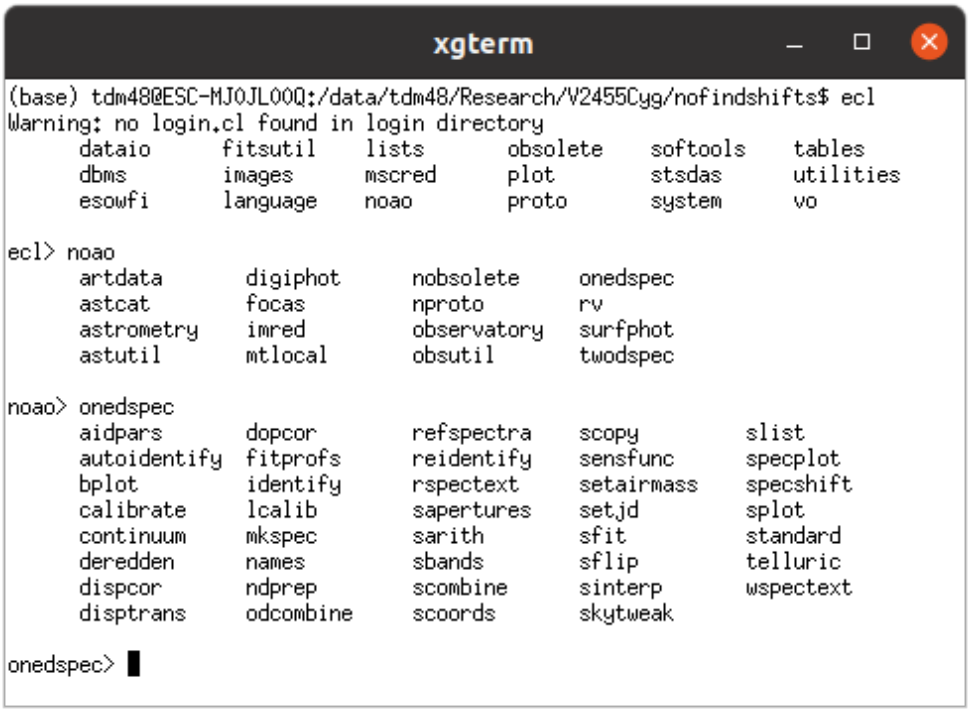

Figure 2.7 IRAF window depicting the ONEDSPEC package which contains the RSPECTEXT, WSPECTEXT, SPLOT, and SCOPY scripts used in the file conversion process as well as several other scripts not used.

A good test to see if the data is working correctly is to try plotting it with the SPLOT command that is also located in the ONEDSPEC package, and it is working if the x axis is defined in angstroms instead of pixels. It is worth noting at this point that if attempting to fit a specific segment of data instead of the entire curve, then this is the best place to cut up the data. This is completed most easily at this point since the data is most accessible while in the Excel document, and saving just that specific segment in the .text file will allow for the easiest separation of the data. One final note in the conversion of .text to .fits files is that the RSPECTEXT command will naturally connect any gap in the data with a line from each end point to the other end. This is beneficial for completing a Fourier Transform since it is considerably easier to fit to a connected curve than trying to make a fit that works with three separate, disjoint segments.

2.2.1 FXCOR Package

Upon completing the data reduction and conversion process it is now possible to extract the radial velocities using the FXCOR command located in the RV package of IRAF. This article (Alpaslan 2009) provides an in depth instruction manual for how to use the FXCOR package. FXCOR accepts a template and object spectra from which it completes a Fourier cross-correlation of both images and detects the difference in spacing between the two spectra to derive a radial velocity value. The Fourier cross-correlation is essentially a complex Fourier Transform which allows for a direct comparison between two spectras that are shifted slightly different from one another. This detected shift is what is used to determine the change in radial velocity over time. It is important to choose a specific .fits file and use it as the template spectra for all of the other data points to be compared to since FXCOR will be run for each individual spectra.

Within FXCOR there are several different parameters that can be changed in order to detect the most accurate radial velocity values, and the most valuable is the function parameter. These different functions provide several ways to fit the two data files which include gaussian, parabola,

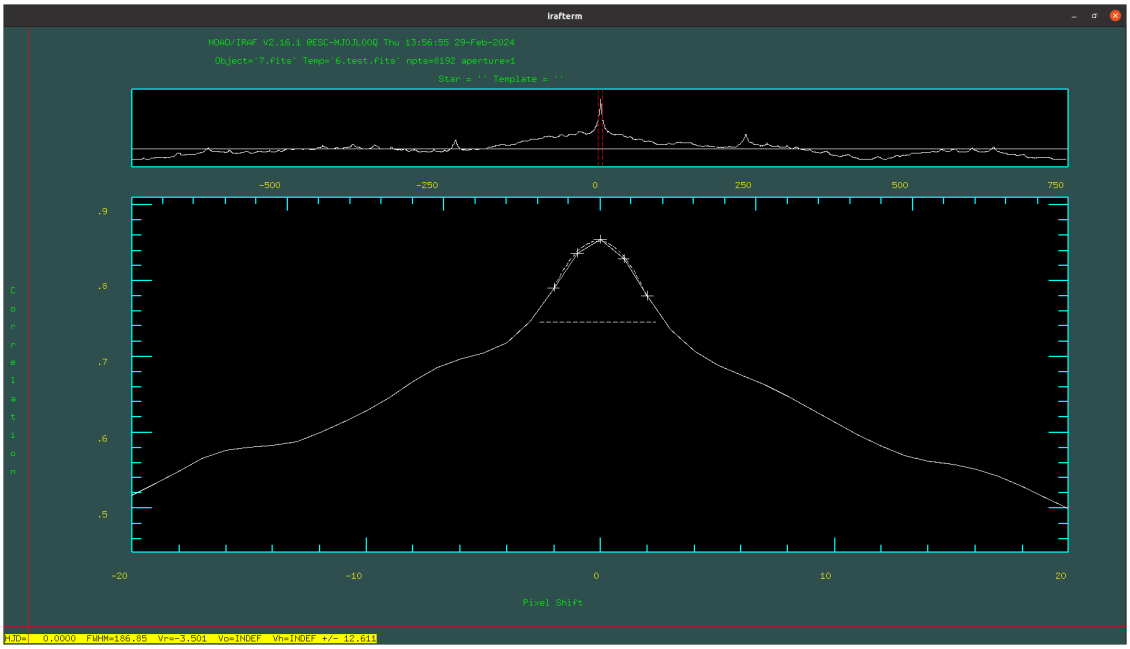

Figure 2.8 FXCOR window depicting the Fourier cross-correlation process with derived radial velocity value and error bars located in the bottom left corner in yellow. The x axis of the graph is the pixel shift and the y axis is the percent of correlation. The best radial velocity results come from fitting only where the correlation is 0.8 or higher

sinc, lorentzian, and center1d. The parabola function has consistently worked the best with the smallest error bars, but the gaussian and sinc are the next best alternatives. Neither the lorentzian or center1d functions have provided actual radial velocity values, but information can be found on them by typing "FXCOR HELP" into the RV package of IRAF. It is possible to see the error values at the bottom left corner of the FXCOR window which helps to identify the overall quality of each fit.

When FXCOR runs it will automatically try to determine the best possible fit, but oftentimes using the g-keystroke to mark the endpoints of a new fit allows to roughly estimate one that aligns better with the data than the original fit. The FXCOR window is centered on a large plot where the x axis is the pixel shift that has occurred and the y axis is the correlation of what percentage of the fit lines up. The FXCOR HELP function located within IRAF recommends to try and align the fit

within a correlation range that is greater than 80% in order to optimize the radial velocity value detected. This can be seen in Figure 2.8 which is an example of the FXCOR window with a radial velocity detected using a parabola function.

We have found that it is time well spent to determine the best possible template spectra since all of the other spectra will be measured directly from this one. Also, since the FXCOR process is shifting the data of two images from one another, it subtracts the radial velocity of the star as it moves in relationship to Earth. This means the radial velocity values detected are only from the change in size of the star throughout its pulsation cycle. Finally, as stated above, it is important to remember to not perform any pixel shifts in the data reduction process that cleans the data since it will effectively erase the radial velocity values that we are trying to detect.

Chapter 3

Results

The data reduction process above explains how to extract radial velocity values from near-infrared spectroscopic data, and this process must be repeated for each data point used in the figures below. To accurately depict the pulsation curve, our research group completed the reduction process with thirty different data points spread out throughout the observation period. Every data point below was created by using four raw images at the start of the reduction process since using any less would result in data with too high of a signal-to-noise ratio.

3.1 Radial Velocity Figures

Our team was unsure of whether a specific part of the data would most accurately create radial velocity curves as this was an initial study of radial velocity detection using spectroscopic data. This led us to experimenting several different wavelength ranges to see what led to the best possible results. Figure 3.1 here depicts the different hydrogen absorption lines that regularly appear in the data from V2455 Cyg. Since the Fourier cross-correlation works specifically with these hydrogen lines, it is possible that different absorption lines would lead to a variety of results.

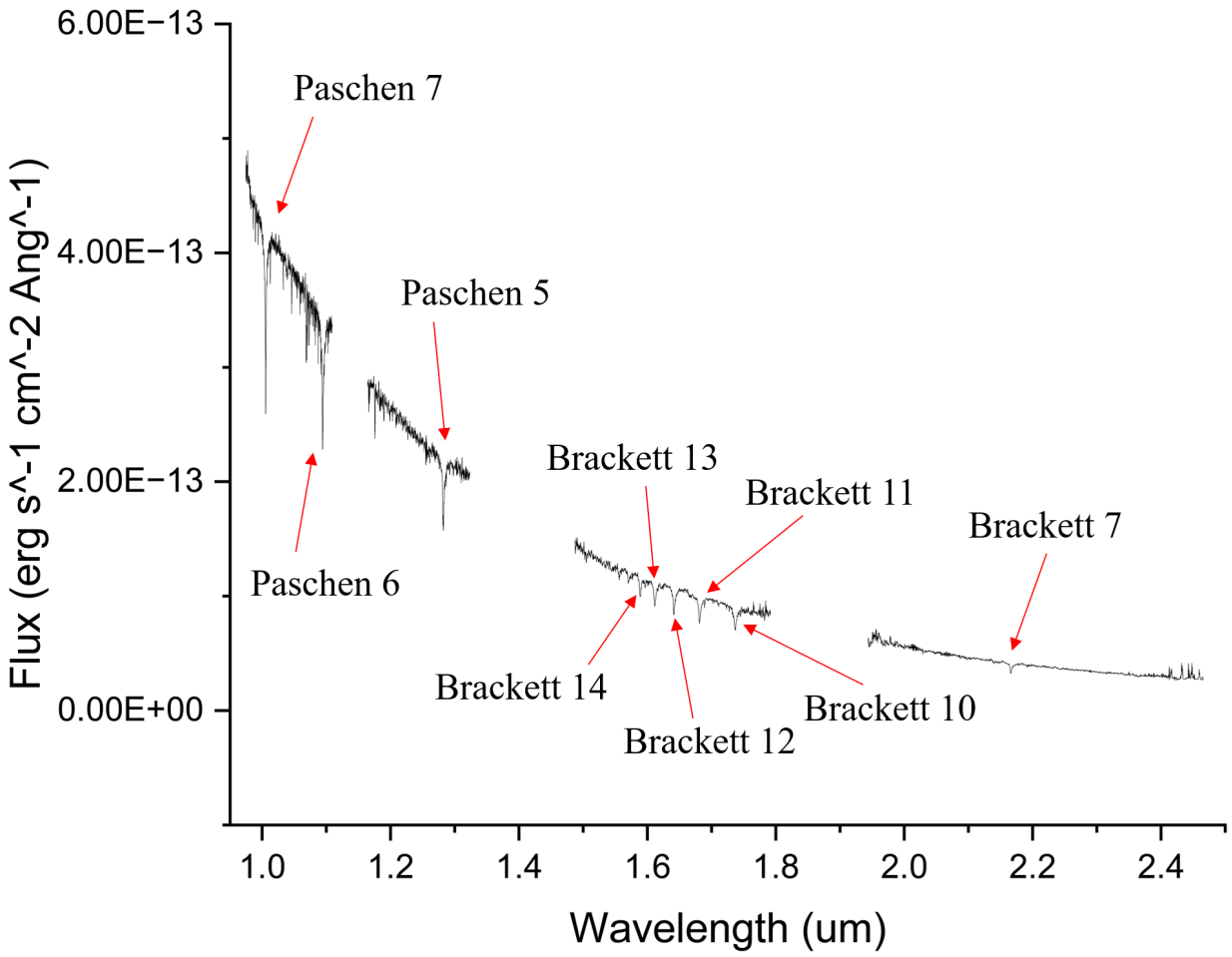

Figure 3.1 Locations of known hydrogen absorption features located on a stellar blackbody curve. In order to determine the best possible detection of radial velocities, FXCOR was run using four separate sections of the data: Paschen Lines 6-7 located in the J Band, Paschen Line 5 located in the J Band, Brackett Lines 10-14 in the H Band, and the entire spectra which contains Paschen Lines 5-7 and Brackett Lines 7 and 10-14.

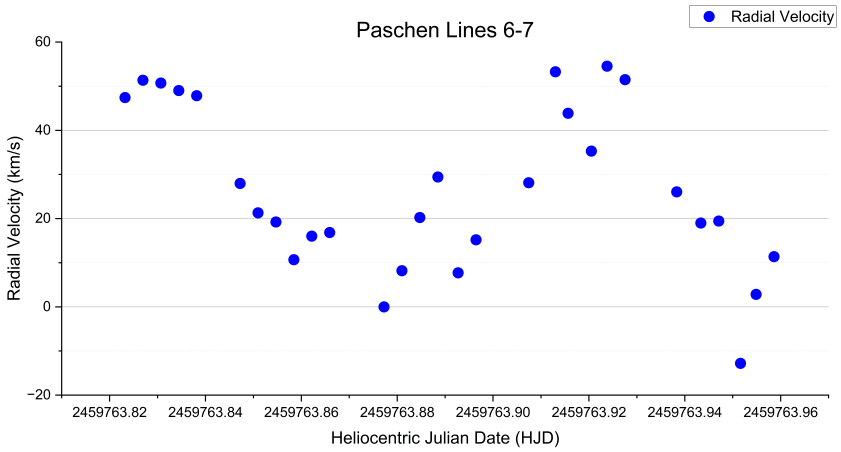

Figure 3.2 Detected radial velocity curves of V2455 Cyg from Paschen Lines 6-7 located in the J Band that were calculated using a Fourier cross-correlation.

Ultimately, our research team decided to work on four separate parts of the data which were naturally divided because of the gaps in the data formed by the atmospheric noise. The first section we used is the top most left side of Figure 3.1 that contains both the Paschen 6 and 7 lines, and it's radial velocity curve can be seen in Figure 3.2. The next section we tried contains Paschen Line 5 and is just to the right of the first section used in Figure 3.1. Both of these two fits are located within the H Band and the second set of radial velocity values are depicted in Figure 3.3. The third place that we tried fitting the data to was in the H Band, which is where the majority of the Brackett Lines are located. Figure 3.4 depicts their radial velocity curve. The final section containing Brackett Line 7 had too much noise and too small of a spectral line to accurately be used. Thus, the final data range we used was trying to fit the entire spectra covering both Brackett and Paschen lines, and it's radial velocity curves are defined with Figure 3.5.

We had anticipated that the data using the entire spectra would create the most reliable radial velocity values since it has the largest number of spectral lines to be used in the Fourier cross-correlation. However, this is not reflected in our data because of the distinct gaps that are formed from the noise in the atmosphere. The software struggled to complete the fits here because Fourier

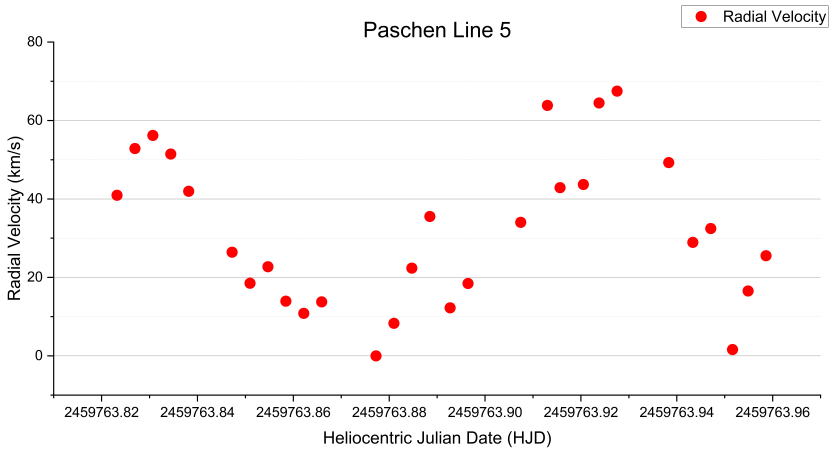

Figure 3.3 Detected radial velocity curves of V2455 Cyg from Paschen Line 5 located in the J Band that were calculated using a Fourier cross-correlation.

Transforms have a hard time interpreting data when it abruptly changes. The J, H, and K bands are linearly connected together in our data, but the connecting lines could be different enough from the actual data for the software to have a harder time fitting them. Even with these attempts, it can be seen that Figure 3.5 has a larger range of radial velocity values than the other figures. This could be in part from a lack of noise in the connecting lines that linked each band together, so the software mistook them to also be spectral features.

The data that we found containing the most distinctive curve is actually depicted in Figure 3.4 since it uses the most spectral lines all closely placed to one another. The values come out so clean because of the several existing spectral lines used to complete the fit, and since this segment of data has very little noise throughout it. This results in FXCOR only detecting the known absorption lines and nothing else in the data.

Our group attempted using the find shifts function in the telluric correction step of the data reduction process to limit the atmospheric influence, but this performs a pixel shift with the data that essentially eliminates the accuracy of the radial velocity fits. Thus, it is necessary to use the data with atmospheric noise which can also limit the accuracy of the radial velocity curves, but to a

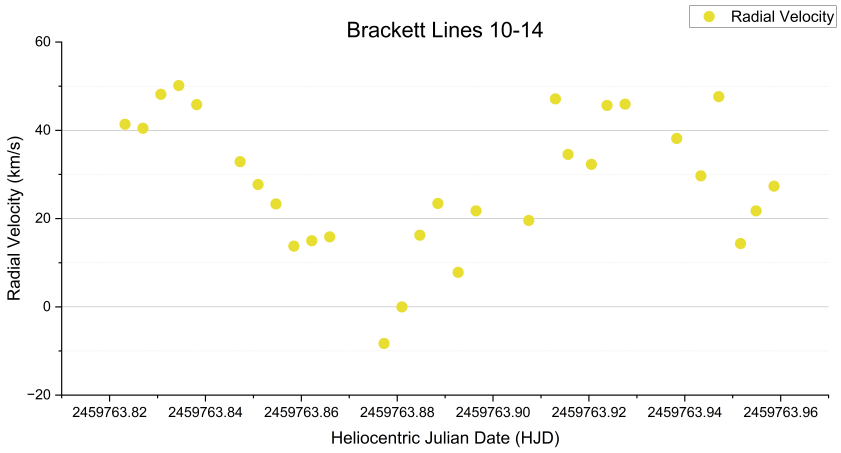

Figure 3.4 Detected radial velocity curves of V2455 Cyg from Brackett Lines 10-14 located in the H Band that were calculated using a Fourier cross-correlation.

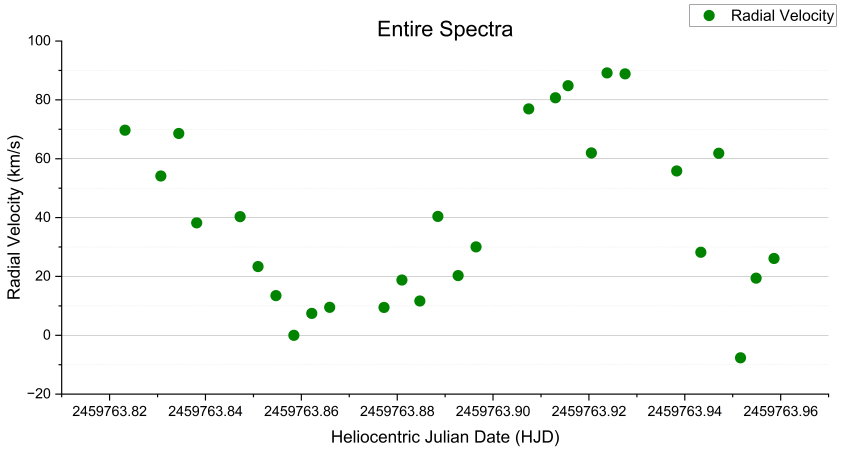

Figure 3.5 Detected radial velocity curves of V2455 Cyg from Paschen Lines 5-7 and Brackett Lines 7 and 10-14 located in the J, H, and K Bands that were calculated using a Fourier cross-correlation.

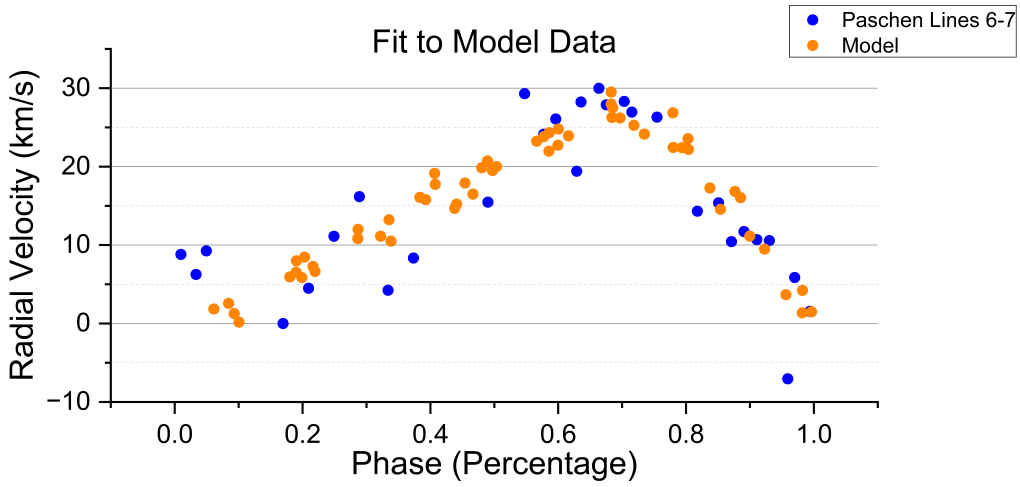

Figure 3.6 Comparison of radial velocity values between optical data and the curves extracted from the Paschen Lines 6-7. Both radial velocities were observed from the δ scuti star, V2455 Cyg. The actual radial velocity values from the data points collected in the near-infrared were scaled to better align with the optical data points, allowing for a closer comparison of the shape between the two curves.

lesser extent. In order to make sure that we were detecting actual radial velocity curves that aligned with the published ephemeris, we compared it with radial velocity curves that were detected from optical, photometric data of the same star.

3.2 Comparison with Optical Data

One way that our team has been able to determine the accuracy of our radial velocity curves has been to compare them to optical data that is also from V2455 Cyg. Figures 3.6, 3.7, 3.8, and 3.9 all directly compare our radial velocity values with the optical data depicted with the orange curve. The data used to form the orange curve was provided by my advisor, Dr. Eric Hintz, and they detected radial velocity values using a different, more reliable process than FXCOR. These figures appear different than the original radial velocity figures because the x axis is defined as the percentage of the period of V2455 Cyg instead of time. This means the figures are depicting one complete period

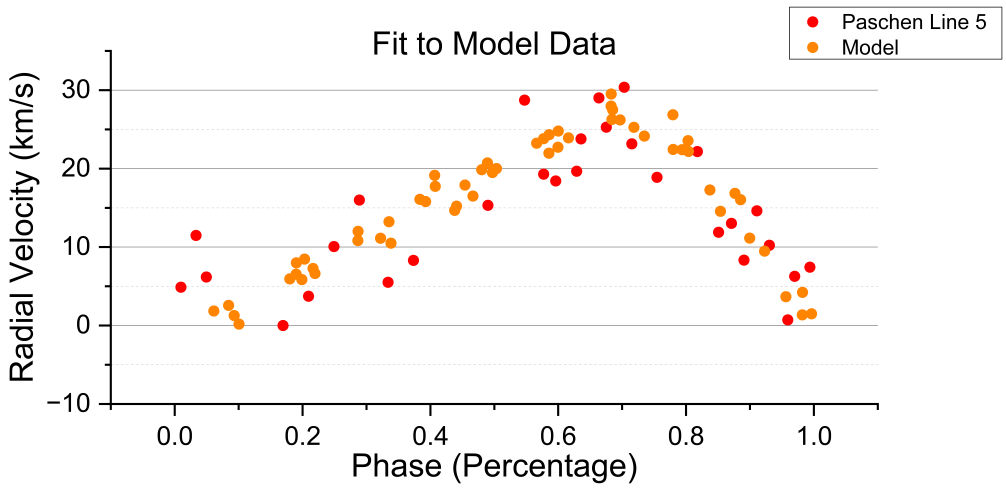

Figure 3.7 Comparison of radial velocity values between optical data and the curves extracted from the Paschen Line 5. Both radial velocities were observed from the δ scuti star, V2455 Cyg. The actual radial velocity values from the data points collected in the near-infrared were scaled to better align with the optical data points, allowing for a closer comparison of the shape of the detected period.

starting at zero percent and progressing up to one hundred. Also worth noting in this section is that our detected radial velocity values are scaled down to line up with the optical data since their range of radial velocity values are about one quarter of what we detected in the near-infrared.

Although the radial velocity values that we detected were significantly larger than the contemporary data, there is a positive result that our data very closely resembles the shape of the optical data. It is common in δ scuti stars that the peak brightness in the pulsation will not occur exactly in the middle of the period, but it will have a more gradual increase in brightness followed by a distinct drop. This creates a sawtooth shape that is clearly reflected in Figures 3.6, 3.7, 3.8, and 3.9. Since both of the data sets are creating very similar shapes it confirms that our research process is detecting genuine radial velocity curves forming from V2455 Cyg's pulsations.

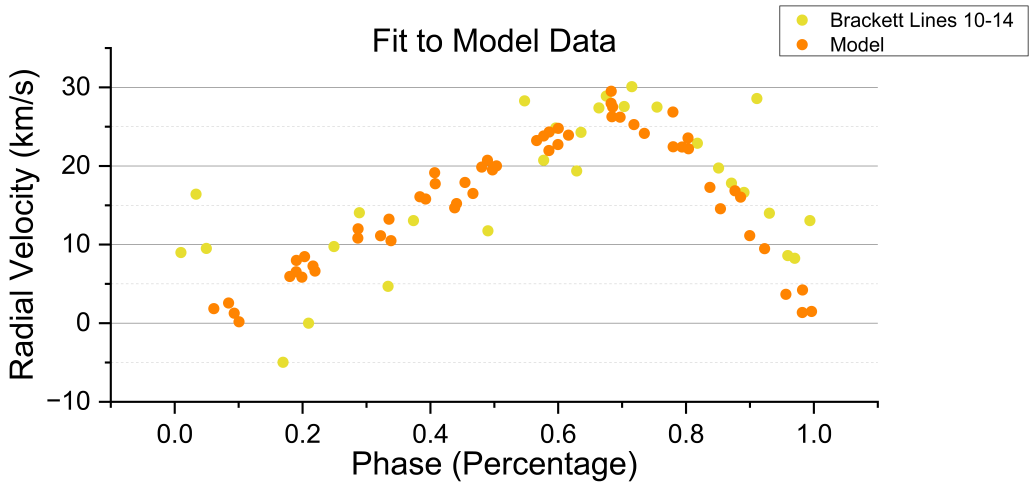

Figure 3.8 Comparison of radial velocity values between optical data and the curves extracted from the Brackett Lines 10-14. Both radial velocities were observed from the δ scuti star, V2455 Cyg. The actual radial velocity values from the data points collected in the near-infrared were scaled to better align with the optical data points allowing for a closer comparison of the shape of the detected period.

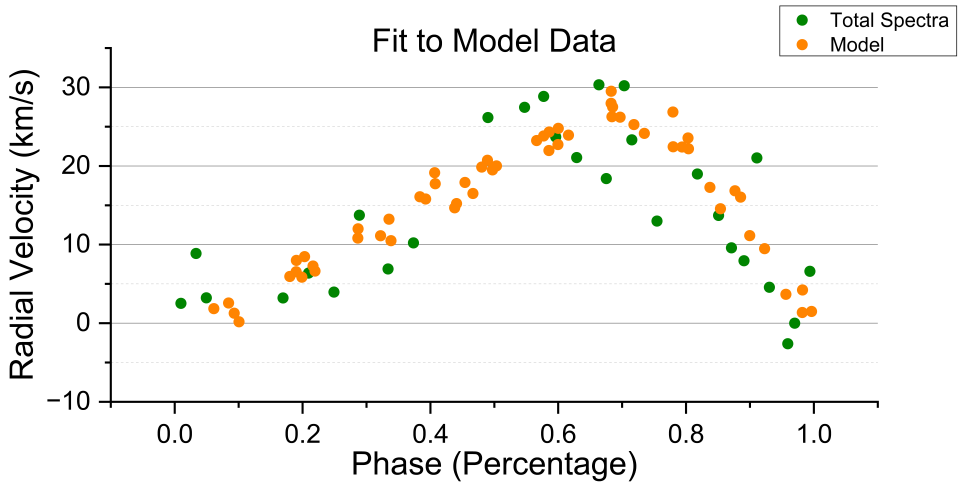

Figure 3.9 Comparison of radial velocity values between optical data and the curves extracted from the Paschen Lines 5-7 and Brackett Lines 7 and 10-14. Both radial velocities were observed from the δ scuti star, V2455 Cyg. The actual radial velocity values from the data points collected in the near-infrared were scaled to better align with the optical data points, allowing for a closer comparison of the shape of the detected period.

Chapter 4

Discussion

Much of the research completed throughout this paper has not been attempted beforehand at Brigham Young University which means there is considerable room for improvement moving forward. The night that V2455 Cyg was observed was one of the first times that students in our research group had used the 3.5 meter telescope remotely, and the significance of using reliable standard stars for the data reduction process had not been realized yet. Similarly, this data was not collected with the sole purpose of being used to detect radial velocities which would involve taking calibration frames periodically throughout the night. It has been a great success at having achieved this much information with the data and their lies great possibilities to build on top of what has been done so far.

4.1 Determining Error Limits

More accurately determining the error bars is the next key problem to solve in the radial velocity detection process as it will provide validity to the pulsating curves. Currently, the radial velocity curves detected in V2455 Cyg directly align with the published ephemeris for the star, but the actual magnitudes throughout the curve vary greatly depending on each figure. This can potentially

be because our data collection process did not include taking the calibration images periodically throughout the night which could have provided more accurate data to begin with.

Another potentially useful way of finding more accurate error values could be within the parameters for FXCOR. There lies the ability of selecting a function where the most reliable options are parabola, gaussian, and sinc. In general, the parabola function has been the most cooperative with our data, and it is possible to refit the model made by the function by using the g-keystroke. With trial and error it is possible to create different fits with corresponding error bounds, and this is the most likely key to confirming radial velocity values being as accurate as possible. It is best to determine the bounds of each model beforehand since having consistency throughout the entire process will result with the best final data as possible.

4.2 Collaborative Data Comparison

As stated in the section above, one of the most significant current challenges is determining the accuracy of the detected radial velocity curves, but comparing results with other methods of determining radial velocities does help put things into a better light. Both (Balona & Laney 2003) and (Guiglion et al. 2013) have performed similar research where they use spectroscopic data to detect changing radial velocities in stars. Similarly, the optical data that was provided by my advisor provides value since it confirms that what we are finding exists in multiple sources. Although none of these other sources are completing identical work as seen in this paper, they provide new insights and function as ways to check that our results are accurate.

By looking at our and the optical radial velocity curves side by side in the results above, it is very clear that both data sets form a very similar shape. They both gradually rise for nearly three quarters of the period and then in the last quarter they have a very distinct drop back to the starting value. This shape is common throughout δ scuti stars and provides validity to the data that has been

collected. The biggest difference still remaining is that the radial velocity values are significantly higher in the near-infrared, but that could partially be true since we are observing a different part of the electromagnetic spectrum. The Paschen and Brackett lines form from higher energy levels than Balmer and Lyman lines which form in the optical range. That means the near-infrared data could be reflecting a different part of the atmosphere that has larger changes in radial velocity.

4.3 Future Research

The research covered in this paper is focused specifically on detecting the radial velocity of a singular δ scuti star over its pulsation period, but this has the potential to be used in several related fields. Provided below are some of the top ways that radial velocity detection through spectroscopic data can be used in future research projects.

4.3.1 Cepheid Stars

As mentioned in the Introduction, cepheids vary from δ scuti stars since they have a longer period that can last several days or up to a month. Since the star remains cooler for a longer period of time the spectra has more drastic changes that can occur to it throughout its pulsation. In δ scuti stars it is common to only detect the change in shape and size of spectral lines, but it is possible for molecules to form in the atmospheres of cepheid stars. This is explained in (Call et al. 2024) where they detect the formation and deformation of carbon monoxide and cyanide molecules during the pulsation period.

Since these particles are detected in the spectra, it is possible to directly observe how at different times over the pulsation period that they will form, grow in magnitude, and eventually dissolve. With this information, it would be possible to use the FXCOR function on these spectral features as they change over the period. This has yet to be tested, but potentially could provide a new and

interesting path to detecting radial velocities. There is the possibility that since this is a bit more technical than a hydrogen absorption line changing in width, that FXCOR will have a harder time piecing together a successful fit, and with the longer pulsation time, it will be necessary to collect data over a period of nights to accurately depict the curve instead of a single night.

4.3.2 Stellar Atmospheres

As we continue to narrow the range of radial velocity error bounds, there is reason to believe that this information can be used to create more accurate models of stellar atmospheres. Brackett and Paschen lines are the most common feature found throughout the spectroscopic data since the atmosphere of a star is one of the few places in the universe with the necessary conditions for them to occur. These lines are formed as hydrogen is ionized from extreme temperatures and pressure. A Paschen line forms when a photon is absorbed by a hydrogen atom and it results in an electron being pushed into an energy shell of n=3. Similarly, the Brackett lines are formed when an electron is at an energy shell of n=4, which means they actually are formed from higher energy photons than the Paschen lines.

Since Brackett and Paschen lines form at different energy levels, this implies that the photons have different amounts of energy depending on where they are located within the star. A hotter part of the star should contain more energy which means that is where Brackett lines would be most likely to exist as compared to Paschen lines. It is also worth considering that we detect only the photons that are located in the atmosphere of a star since the interior is not visible to telescopes. This means the different hydrogen absorption lines could potentially be reflecting different depths of the stellar atmosphere, and as radial velocity detection becomes more accurate, a discrepancy might start to form because the star shrinks and grows at different rates with different atmospheric depths. This would significantly help our understanding of stellar modeling to know if a star changes in size as one continuous mass or if it changes in layers like a wavefront moving across a pond.

4.4 Conclusion

Considerable information has been collected by studying the changing radial velocity values of V2455 Cyg over the space of a single half night. This was achieved by performing a Fourier cross-correlation on spectroscopic data that had been reduced using the *Spextools* software. The previously unused research process has opened the door for projects moving forward that will be able to more accurately detect radial velocities in similar pulsating stars. With the clear results existing from a single night's observations, hopefully there will be time set apart in the future for similar projects to build off of the foundation that has been established.

Studying stars using near-infrared spectroscopy provides an understanding and perspective that is much broader than simple photometric observations. As scientists continue to work on understanding the way that stars grow and evolve, this information can help supply a missing piece of the puzzle by better acquiring accurate radial velocity curves. This has the potential to illustrate the way that different parts of a star's atmosphere can change throughout its pulsation. Figuring out these details can help scientists provide answers to the bigger questions involved with stellar evolution and star formation.

Bibliography

Alpaslan, M. 2009, arXiv e-prints, arXiv:0912.4755

Balona, L. A., & Laney, C. D. 2003, MNRAS, 344, 242

Call, S. G., Hintz, E. G., Ardern, S., Scowcroft, V., & Morrell, T. D. 2024, arXiv e-prints, arXiv:2401.01318

Cushing, M. C., Vacca, W. D., & Rayner, J. T. 2004, PASP, 116, 362

Guiglion, G., et al. 2013, A&A, 550, L10

Handler, G. 2009, in American Institute of Physics Conference Series, Vol. 1170, Stellar Pulsation: Challenges for Theory and Observation, ed. J. A. Guzik & P. A. Bradley, 403–409

Hubble, E. 1988, in The Early Universe: Reprints, ed. E. W. Kolb & M. S. Turner, 9

Lafler, J., & Kinman, T. D. 1965, ApJS, 11, 216

Ostadnezhad, S., Forozani, G., & Ghanaatian, M. 2020, Research in Astronomy and Astrophysics, 20, 105

Scoresby, C., Turner, S., & Stephens, D. 2023, in American Astronomical Society Meeting Abstracts, Vol. 55, American Astronomical Society Meeting Abstracts, 203.10

Tody, D. 1986, in Society of Photo-Optical Instrumentation Engineers (SPIE) Conference Series, Vol. 627, Instrumentation in astronomy VI, ed. D. L. Crawford, 733

Tonry, J., & Davis, M. 1979, AJ, 84, 1511

Vacca, W. D., Cushing, M. C., & Rayner, J. T. 2003, PASP, 115, 389

Wilson, J. C., et al. 2004, in Society of Photo-Optical Instrumentation Engineers (SPIE) Conference Series, Vol. 5492, Ground-based Instrumentation for Astronomy, ed. A. F. M. Moorwood & M. Iye, 1295–1305

Index